# Observing Herbig Ae/Be Stars with ISO-LWS

Elisabetta Tommasi

*ISO Science Operation Centre, Villafranca, P.O. Box 50727, 28080 Madrid, Spain*

Teresa Giannini

*IFSI-CNR, C.P.27, 00044 Frascati, Italy*

Dario Lorenzetti

*Osservatorio Astronomico di Roma (Italy)*

Brunella Nisini, Paolo Saraceno

*IFSI-CNR, C.P.27, 00044 Frascati, Italy*

Howard Smith

*Harvard-Smithsonian Center for Astrophysics - Cambridge (USA)*

**Abstract.** We present far infrared observations of a sample of Herbig Ae/Be stars, obtained with ISO-LWS in the low resolution configuration. The data reduction procedure is discussed along with the criteria followed for line detection. The continuum data are compared with IRAS detections and the locus of these stars in a new ISO col-col diagram is identified; the fluxes of all the detected lines, both on-source and in the adjacent field positions, are reported.

## 1. Observations

A sample of 10 Herbig Ae/Be stars has been observed with the Long Wavelength Spectrometer (LWS) on board of Infrared Space Observatory (ISO); see Lorenzetti et al. (this issue) for a description of the sources.

The observations were carried out with the LWS AOT01 full grating scan mode (i.e. range=43-196.7$\mu m$, $\lambda/\Delta\lambda\sim200$, FOV$\sim$80"), using the "fast scanning" option and an oversampling of 4 (Clegg et al. 1996). In order to evaluate any possible contamination arising in the neighbourhood of the sources, all the observations are carried out by doing different pointings, sometimes in form of a raster map. The Journal of observations is given in Table 1.

The ISO-LWS data are affected by various systematic effects such as glitches due to impacts of cosmic rays, non-linear detector behaviour, differences between overlapping spectra, fringes and uncertainty in the beam size (Trams, 1997); the current status of data reduction and calibration allows to correct these ef-

Table 1. Journal of observations.

| source | date | orbit | raster points | $t_{int}$(sec) | number of scans |
|---|---|---|---|---|---|
| LKH$\alpha$ 198 | 24Aug96 | 282 | – | 1.6 | 4 |
| LKH$\alpha$ 198 off | 24Aug96 | 282 | 2×1 (180$''$) | 1.6 | 4 |
| V376 Cas | 24Aug96 | 282 | – | 1.6 | 4 |
| HD97048 | 3Aug96 | 261 | – | 3.2 | 8 |
| HD97048 off | 3Aug96 | 261 | 2×1 (100$''$) | 1.6 | 4 |
| IRAS 12496-7650 | 11Mar96 | 115 | – | 7.6 | 19 |
| IRAS 12496-7650 flow | 11Mar96 | 115 | 3×3 (100$''$) | 0.45 | 3 |
| CoD-42$^o$ 11721 | 9Feb96 | 84 | 3×1 (100$''$) | 0.45 | 3 |
| R CrA | 15Oct96 | 334 | – | 2.4 | 6 |
| R CrA off | 15Oct96 | 334 | 3×1 (100$''$) | 6 | 15 |
| PV Cep | 28Jul96 | 255 | – | 6 | 15 |
| PV Cep flow | 28Jul96 | 255 | 2×1 (180$''$) | 2.8 | 7 |
| V645 Cyg | 5Aug96 | 263 | 3×1 (100$''$) | 1.6 | 4 |
| LKH$\alpha$ 234 | 15Feb97 | 457 | – | 6 | 15 |
| NGC 7129 flow | 17Nov97 | 367 | 2×6 (100$''$) | 1.6 | 4 |
| MWC 1080 | 25Aug96 | 283 | – | 2.8 | 7 |
| MWC 1080 flow | 25Aug96 | 283 | 2×2 (100$''$) | 1.6 | 4 |

Note: $t_{int}$ is the integration time per spectral sample

fects even if some problems are still under investigation and great efforts are in progress to improve the quality of the data.

## 2. Data reduction.

The raw data extracted from the telemetry were processed with the last version of off-line pipeline (OLP V6), which corrects for the detector responsivity drift and performs wavelength and flux calibration. The flux calibration is based on observations of Uranus, resulting in an extimated accuracy of $\sim 30\%$ (Swinyard et al. 1996); the wavelength calibration accuracy is a quarter of the resolution element, i.e. $0.07\mu m$ in the range 43-90$\mu m$ (SW) and $0.15\mu m$ in 90-197$\mu m$ (LW).

The product of the off-line pipeline is a series of repeated spectral scans, each of them composed of ten sub-spectra corresponding to the ten detectors; so the subsequent steps of the data reduction are the following: averaging the different spectral scans using the median clipping method that removes outlying values due to the impacts of cosmic rays; removing the fringes; re-scaling the ten sub-spectra to the average of the overlapping regions.

## 3. Results

*Continuum.* The resulting spectra for 2 of the 10 sources are presented in Figure 1 (*left*) along with their OFF positions.

In Table 2 the comparision between the results of the ISO-LWS observations and IRAS-PSC fluxes (Berrilli et al., 1992) is shown. Within the errors associated with the data, all the values are in agreement; some major differences can be due to the different beams of the two instruments as all our sources are spatially extended. In the table the new detections at 100$\mu m$, not given in the IRAS-PSC, are emphasized.

Table 2. Comparison IRAS – ISO-LWS

| source | IRAS 60$\mu m$ (Jy) | IRAS 100$\mu m$ (Jy) | ISO–LWS* 60$\mu m$ (Jy) | ISO–LWS* 100$\mu m$ (Jy) |
|---|---|---|---|---|
| LKH$\alpha$ 198 | 127(140†) | 183(207†) | 134 | 159 |
| V376 Cas | 127(138†) | 183(198†) | 159 | 146 |
| HD97048 | 70 | <250 | 78 | **71** |
| IRAS12496-7650 | 105 | 87 | 107 | 93 |
| CoD-42$^o$ 11721 | 1918 | 2213 | 1809 | 1770 |
| R CrA | 608 | 1206 | 779 | 1201 |
| PV Cep | 50 | 58 | 43 | 45 |
| V645 Cyg | 371 | 455 | 571 | 562 |
| LKH$\alpha$234 | 592† | – | 793 | **1011** |
| MWC 1080 | 147 | – | 196 | **270** |

Notes: * values are obtained computing the convolution of the averaged scans with the IRAS filters for both on-source and off-source measurements and taking the difference; † fluxes from IRAS ADDSCAN

The novelty of ISO-LWS spectrophotometry is the opportunity to have the spectral shape of the sources up to $\approx 200\mu m$. Aiming to have a simple diagnostic tool for unraveling the photometric behaviour of objects in different evolutionary stages, we define the ISO colours as $[\lambda_1 - \lambda_2] = Log(F_\nu(\lambda_2)/F_\nu(\lambda_1))$ (where $F_\nu(\lambda)$ is the flux density in Jansky obtained averaging the LWS spectral values in a range of $5\mu m$ around $\lambda$) and we plot in Figure 1 (*right*) the ISO colours $[60 - 100]$ *vs* $[100 - 170]$. We note that the Herbig Ae/Be stars cluster in a well defined locus defined by the colours $0 < [60 - 100] < 0.25$, $-0.25 < [100 - 170] < 0$; this is consistent with envelopes whose temperatures range between 90K and 40K, as expected from the spectral energy distributions of these sources.

*Lines.* The line analysis has been performed on the defringed single detector subspectra; we subtract a polynomial function fitting the continuum and performe a best fit with a single or double gaussian function.

The following criteria have been adopted to ascertain the detection of a line: *i)* $\mid \lambda_{obs} - \lambda_{lab} \mid \leq 0.07$(SW) or 0.15(LW); *ii)* $fwhm = 0.29 \pm 0.07$ (SW) or

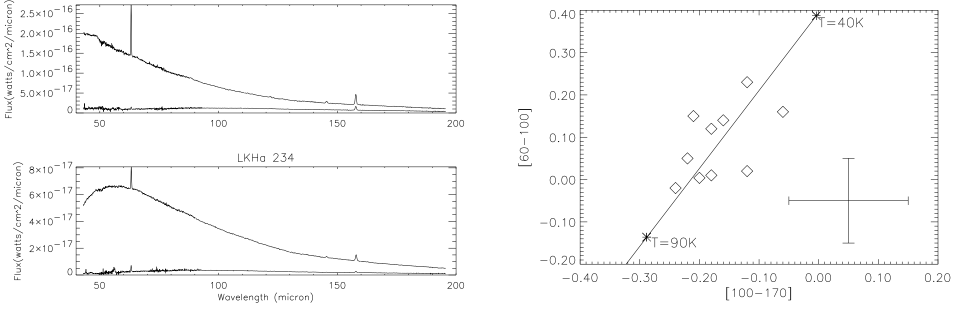


Figure 1. (*left*) Examples of resulting spectra; (*right*) ISO col-col diagram (the line represents the blackbody temperature scale)

Table 3. Line intensities.

| source | [OI]63.2 | [OI]145.5 | [CII]157.7 | [OIII]51.8 | [OIII]88.4 | [NII]121.9 |
|---|---|---|---|---|---|---|
| | **Atomic lines** | | | | | |
| | F (ΔF) $10^{-19} W/cm^2$ | | | | | |
| LKH$\alpha$198 | 4.1(0.5) | <0.8 | 5.6(0.3) | – | – | – |
| V376 Cas | 2.2(0.7) | <0.6 | 5.4(0.4) | – | – | – |
| off | 1.7(0.6) | <0.3 | 3.4(0.1) | – | – | – |
| HD97048 | 1.9(0.3) | <0.2 | 0.9(0.1) | – | – | – |
| off | <1.3 | <0.2 | 0.3(0.1) | – | – | – |
| IRAS12496 | 4.3(0.3) | 0.31(0.08) | 0.45(0.1) | – | – | – |
| off | <3 | <0.4 | 0.47(0.09) | – | – | – |
| CoD-4211721 | 400(6) | 32(3) | 205(3) | ≤17 | 14(3) | 15(3) |
| off | 27(2) | <2 | 76(2) | <20 | 7(2) | 11(1) |
| V645 Cyg | 9.6(1) | <0.6 | 16(1) | <3.9 | 5(1) | – |
| off | <2 | 0.4(0.1) | 6.7(0.2) | <4 | 8.5(0.4) | – |
| R CrA | 58(1) | <4.3 | 3(1) | – | – | – |
| off | 2.1(0.3) | 0.3(0.1) | 0.7(0.1) | – | – | – |
| PV Cep | 2.1(0.3) | <0.1 | 0.36(0.07) | – | – | – |
| off | <1 | <0.1 | 0.4(0.1) | – | – | – |
| LKH$\alpha$234 | 55(1) | 6.7(0.4) | 32.5(0.6) | – | – | – |
| off | 2.2(0.3) | <0.2 | 2.8(0.4) | – | – | – |
| MWC1080 | 14.3(0.6) | 1.2(0.4) | 13.5(0.4) | – | – | – |
| off | 6.0(0.5) | 6.7(0.4) | 32.5(0.6) | – | – | – |

| $\lambda$ ($\mu m$) | Line | IRAS12496 | R CrA | LKH$\alpha$234 |
|---|---|---|---|---|
| | **Molecular lines** | | | |
| | | F(ΔF) ($10^{-19}$ $W/cm^2$) | | |
| 71.2 | OH $^2\Pi_{1/2,J=7/2} \rightarrow {}^2\Pi_{1/2,J=5/2}$ | – | <2.4 | – |
| 79.2 | OH $^2\Pi_{1/2,J=1/2} \rightarrow {}^2\Pi_{3/2,J=3/2}$ | – | 4(1) | – |
| 84.6 | OH $^2\Pi_{3/2,J=7/2} \rightarrow {}^2\Pi_{3/2,J=5/2}$ | – | 9(2) | – |
| 124.2 | CO 21→20 | <0.3 | – | 4(1) |
| 130.4 | CO 20→19 | 0.14(0.05) | – | – |
| 137.2 | CO 19→18 | 0.30(0.05) | 4(1) | – |
| 144.8 | CO 18→17 | 0.42(0.05) | <6.8 | – |
| 153.2 | CO 17→16 | 0.54(0.06) | 5.8(0.9) | – |
| 162.8 | CO 16→15 | 0.46(0.05) | 6.4(0.9) | 3.0(0.7) |
| 173.6 | CO 15→14 | 0.36(0.05) | 5.8(0.6) | 1.6(0.5) |
| 186.0 | CO 14→13 | <0.6 | 4.6(0.6) | 1.3(0.4) |

$0.60 \pm 0.15$ (LW); *iii)* $S/N \geq 3$ where $S$ is the integrated line flux and $N$ is the r.m.s. of the (continuum+line) fit. In Table 3 we present all the detected atomic and molecular lines which fulfill these criteria. We note that all the reported lines are detected for the first time in the Herbig Ae/Be star environments. We refer to Lorenzetti et al. (this issue) for a discussion of these results.

**Acknowledgments.** These observations are part of the Guaranteed Time Program and as such are the results of a jointed effort of all the ISO-LWS team.

## References

Berrilli, F., Corciulo, G., Ingrosso, G., Lorenzetti, D. et al. 1992, ApJ, 398, 254

Clegg, P.E. et al. 1996 *A&A Letters*, 315, L38

Lorenzetti, D., Tommasi, E., Giannini, T. et al. 1997, this issue

Swinyard, B.M. et al. 1996 *A&A Letters*, 315, L43

Trams N. 1997, *ISOLWS Data User Manual*, SAI/95-219/Dc, Issue 4.